

Terahertz imaging and spectroscopy based on hot electron bolometer (HEB) heterodyne detection*

Eyal Gerecht** and Lixing You

Electromagnetics Division
National Institute of Standards and Technology, Boulder, CO 80305

ABSTRACT

Imaging and spectroscopy at terahertz frequencies have great potential for healthcare, plasma diagnostics, and homeland security applications. Terahertz frequencies correspond to energy level transitions of important molecules in biology and astrophysics. Terahertz radiation (T-rays) can penetrate clothing and, to some extent, can also penetrate biological materials. Because of their shorter wavelengths, they offer higher spatial resolution than do microwaves or millimeter waves.

We are developing hot electron bolometer (HEB) mixer receivers for heterodyne detection at terahertz frequencies. HEB detectors provide unprecedented sensitivity and spectral resolution at terahertz frequencies. We describe the development of a two-pixel focal plane array (FPA) based on HEB technology. Furthermore, we have demonstrated a fully automated, two-dimensional scanning, passive imaging system based on our HEB technology operating at 0.85 THz. Our high spectral resolution terahertz imager has a total system noise equivalent temperature difference (NE Δ T) value of better than 0.5 K and a spatial resolution of a few millimeters. HEB technology is becoming the basis for advanced terahertz imaging and spectroscopic technologies for the study of biological and chemical agents over the entire terahertz spectrum.

Keywords: terahertz imaging, terahertz spectroscopy, terahertz receivers, hot electron bolometers, heterodyne detectors, superconducting devices, quasi-optical systems, focal plane arrays.

1. INTRODUCTION

Terahertz radiation (T-rays) can penetrate clothes, dust, smoke, and biological materials better than infrared or visible light can. This penetration capability and T-rays' shorter wavelengths have led to the development of imagers with higher spatial resolution compared with those based on microwaves or millimeter waves. Such applications include terahertz imagers for detecting concealed weapons, illicit drugs, and biological materials. Furthermore, the unique spectra of some materials in the terahertz frequency range have led to the development of ultra sensitive spectrometers both for astrophysical and terrestrial applications. Heterodyne terahertz receivers are well suited for spectroscopic application due to their exceptionally high spectral resolution.

Hot electron bolometric (HEB) mixers, which use nonlinear heating effects in superconductors near their transition temperature, have become an excellent candidate for applications requiring low noise temperatures at frequencies from 0.5 THz to 10 THz. HEB receivers for terahertz frequencies have been developed for the past ten years [1]. Heterodyne HEB detectors can operate throughout the entire terahertz spectrum with higher sensitivity than any other terahertz heterodyne detector. Furthermore, the local oscillator (LO) power requirement of HEB mixers (a few hundred nanowatts) is significantly lower than that of any other terahertz heterodyne detector. Maintaining a low LO power consumption is a major challenge in the de-

*Contribution of NIST, not subject to US copyright.

**gerecht@nist.gov; phone (303) 497-4199; fax (303) 497-3970

velopment of multi-pixel focal plane arrays (FPA) at terahertz frequencies. This is due to the difficulties in producing sufficient LO power output at terahertz frequencies.

We review our high sensitivity HEB technology. A passive heterodyne imaging system consisting of a focal plane array of HEB detectors is currently under development. We chose 850 GHz as one of the operating frequencies for our system because it is one of the atmospheric windows for terahertz radiation and gives relatively high spatial resolution. In principle, we could operate at any terahertz frequency. Lastly, spectroscopic systems covering significant portions of the terahertz spectrum are under development, which take advantage of the exceptional spectral resolution of HEB mixers.

2. HEB TECHNOLOGY

2.1 HEB devices

HEBs are surface superconducting devices with extremely small parasitic reactances, even at the highest terahertz frequencies. HEB devices are able to absorb radiation up to the visible range due to the very short momentum scattering times. The devices change their resistance as the quasi-particles are heated as a function of the incoming energy. HEB devices are fabricated from an NbN film, 3.5 to 4 nm thick, that has been sputtered onto a silicon substrate. Typical device size can range from 2 μm (width) by 0.5 μm (length) to sub-micrometer dimensions. An HEB device integrated with a twin-slot antenna is shown in Figure 1. The device can be matched to the antenna by changing its aspect ratio. HEBs, made of NbN films, have a thermal time constant that is determined by both the rate at which phonons are emitted by the electrons and the escape rate of the phonons from the NbN film to the substrate. NbN HEBs are, therefore, known as phonon-cooled HEBs and can exhibit conversion gain bandwidths of about 4 GHz, while the receiver noise temperature bandwidth can be up to twice the gain bandwidth. An operating temperature range for the HEB devices of 4 K to about 6 K is an advantage compared to most other far-infrared (FIR) devices, which require cooling to sub-kelvin temperatures.

2.2 Quasi-optical coupling

In order to effectively couple the incoming radiations onto the HEB mixer, we designed a quasi-optical system consisting of a silicon lens and a monolithic antenna, as shown in Figure 1. The twin-slot antenna is patterned on a silicon substrate by use of

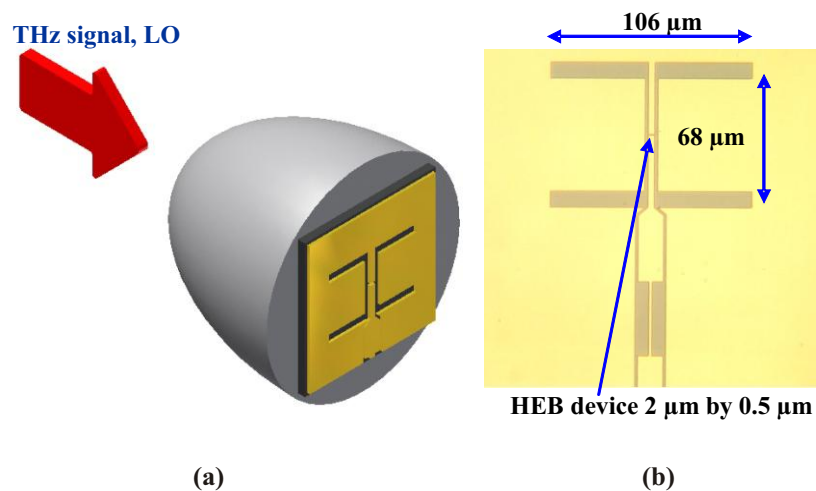


Figure 1: (a) a quasi-optical design illustration; (b) a photograph of the twin-slot antenna. The HEB device in the center of the antenna (arrow tip) is too small to be resolved by the figure.

an electron-beam metallization step followed by a lift-off step. The HEB device is located between the terminals of the twin-slot antenna. The twin-slot antenna has a highly symmetrical and linearly polarized radiation pattern and provides nearly perfect power coupling to the incident Gaussian beam [2]. We have employed three types of antennas: twin-slot antennas, which have a bandwidth of about 20 %, log-periodic antennas, which can be designed to have several octaves of bandwidth depending on the number of teeth, and slot-ring antennas [3], which allow for a more efficient LO injection scheme. We have fabricated and characterized these antennas for a number of frequencies throughout the terahertz spectrum. The terahertz signals couple to the device through an elliptical silicon lens (4 mm in diameter). The lens is a rotational ellipsoid that functions as an aperture antenna, and hence reshapes the far-field radiation pattern. By using a ray-tracing technique, the radiation from the twin slot antenna, placed at the second focus of the lens, becomes a plane wave in the aperture plane outside the lens. By considering the combination of the silicon lens and the twin-slot antenna, the far-field beam has a full-width half-power (FWHP) of about 3 degrees. The fabrication process developed for HEB devices is well suited for fabrication of focal plane arrays (FPAs) based on HEB technology.

2.3 LO sources

The practical available choices of LO sources at terahertz frequencies include FIR lasers operating on a number of discrete spectral lines throughout the terahertz spectrum, and harmonic multiplier sources in the lower terahertz spectrum. We have chosen harmonic multiplier sources as the LO because of their compact size, ease of use, and availability for frequencies in the lower terahertz spectrum. For the higher range, we plan to use quantum-cascade lasers (QCLs) [4] as they develop into a more mature technology. We have deployed a number of commercially available harmonic multiplier sources [5] as the LO signal. Our 850 GHz source consists of a phase-locked oscillator with an output signal at 11.8 GHz and a multiplication chain of 72 times. This particular harmonic multiplier source produces an output power of about 250 μ W, which is sufficient for a small FPA of HEB devices operating in a heterodyne configuration. A tunability of about 10 % was achieved with this multiplier source by replacing the low frequency signal, driving the multiplication chain, with a microwave synthesizer having sub-hertz spectral resolution. In order to combine the LO and the signal radiations for the heterodyne detection scheme, we employ Mylar beam splitters in different polarizations, ranging in thickness from 25 μ m to 6 μ m, reflecting 28 % to 1 % of the incoming LO radiation, respectively.

2.4 Integrated receiver block

In a typical receiver system, the mixer and the low-noise amplifier (LNA) are assembled in separate blocks and connected by coaxial cables. An isolator is often included between the mixer and the LNA to minimize the standing wave between them. Although this configuration has been widely adopted in astrophysical receiver systems, it does not meet the requirement for a compact multi-pixel FPA. Furthermore, the use of isolators limits the IF bandwidth to no more than an octave. To eliminate the use of isolators, we have demonstrated a design for integrating the HEB device and a monolithic microwave integrated circuit (MMIC) LNA in the same block [6]. A multi-section microstrip matching network is employed to achieve broadband coupling between the HEB and the MMIC LNA. The HEB device is located in close proximity to the MMIC chip, which is mounted in a narrow rectangular cavity for the purpose of eliminating possible amplifier oscillations. This particular MMIC LNA has been characterized against standards developed at the National Institute of Standards and Technology (NIST) and, by use of a recently developed measurement technique [7], exhibits noise performance of below 5.5 K from 1 GHz to 11 GHz. To couple the DC signal to the device and extract the intermediate frequency (IF) signal from the device, we use a bias "tee" circuit that is built into the mixer block. Our two-pixel FPA mixer block allows for dual-frequency and dual-polarization operation [8]. Figure 2 shows a photograph of the two-pixel HEB/MMIC integrated mixer block. The two pixels are sep-

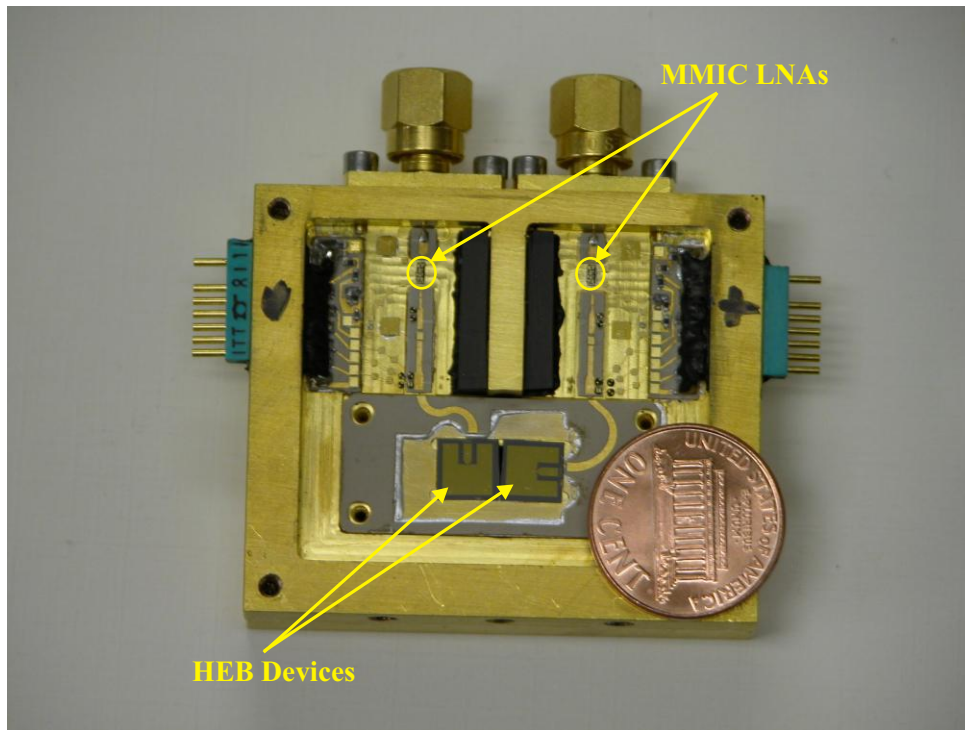


Figure 2: A two-pixel integrated mixer block housing two HEB devices and two MMIC LNAs.

operate and operate independently of each other. SMA coaxial lines and connectors allow us to extract the two IF outputs from the sides of the block, and two connectors provide all DC bias lines for the HEB devices and the MMIC LNAs. The optical configuration of the pixels in the array is of the “fly’s eye” type, which allows ample space for the other components in the focal plane. The performance of this FPA demonstrates the suitability of HEBs as mixer elements in much larger FPA imagers in the future.

3. PASSIVE TERAHERTZ IMAGING

The main components of a passive imaging system include the front-end detecting element, the local oscillator source, the optics design, and the data acquisition system. In order to produce a two-dimensional raster, the heterodyne receiver collects radiation from the scanned object through optical components, such as off-axis parabolic mirrors or dielectric lenses, in both the elevation and azimuth directions by means of a line-by-line sweep (raster scan). Each line of the scan is divided into a number of pixels. The number of pixels and the distance between pixels can be adjusted according to the desired resolution and the size of the target. The total wait period at each pixel is based on the lock-in integration time constant. The signal beam is chopped against a room temperature black-body source and then fed to a lock-in amplifier referenced by the chopping frequency. An automated motion controller, which also functions as a data acquisition (DAQ) system, is used to drive the translators and collect the data in real-time. Figure 3 shows a schematic diagram of a terahertz passive imager.

We have developed a two-dimensional passive terahertz imaging system operating at 850 GHz based on HEB technology. The demonstrated thermal resolution is better than 0.5 K. A spatial resolution of only a few millimeters was also demonstrated. By reducing the noise temperature of the HEB device and cleaning some of the system noise, a substantial improvement in the total imager sensitivity can be achieved. To improve the scanning speed, we are currently developing an imaging

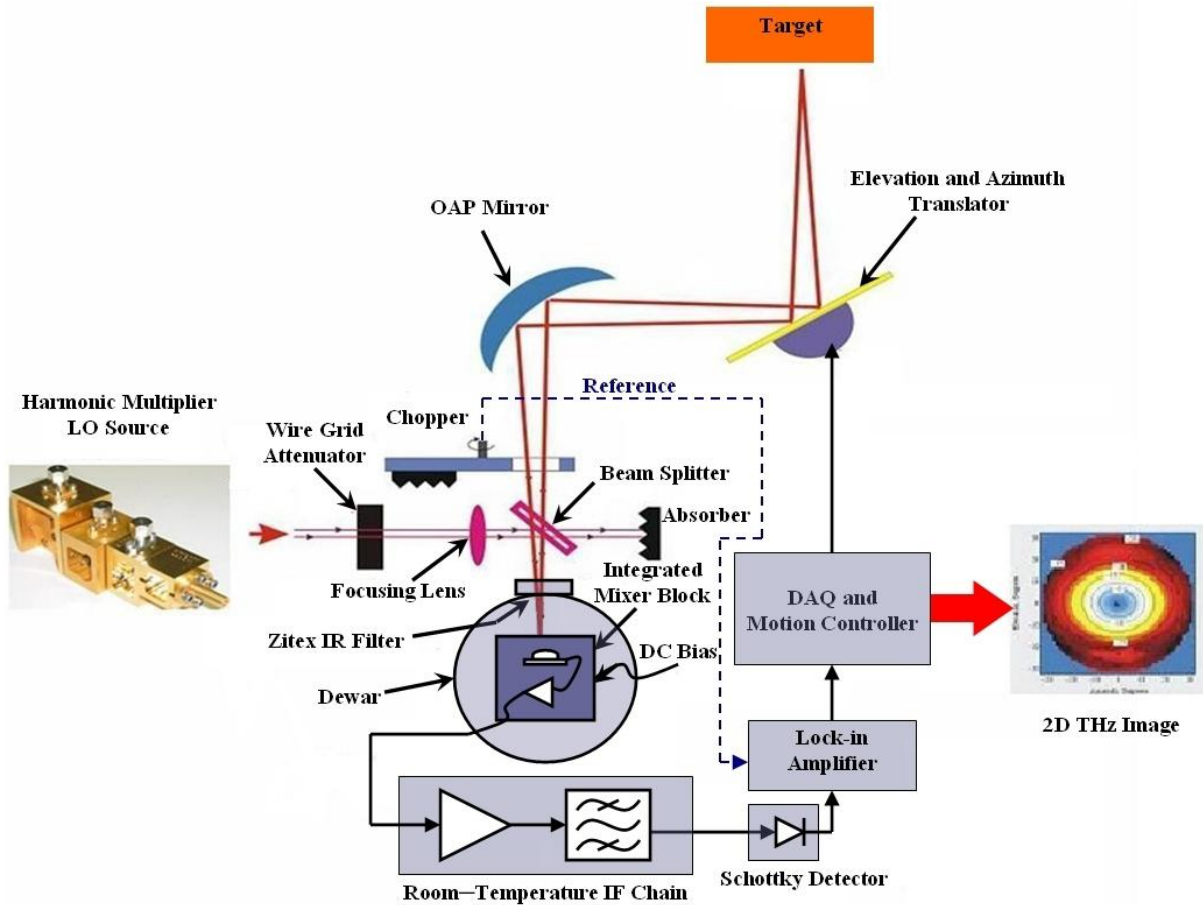


Figure 3: A schematic of a two-dimensional heterodyne terahertz passive imaging system.

system with multiple HEB detectors. An FPA containing three-elements based on HEB mixers and MMIC LNAs has already been demonstrated [6] and delivered to NASA. This design can be extended to a large number of elements. The lenses and HEB devices are arranged in a fly's eye configuration. Such a configuration can produce an angular resolution slightly larger than one diffraction-limited beamwidth (FWHM). Future HEB FPAs will consist of a separate substrate to house the MMIC LNAs. We expect that this new architecture, combined with MEMS micro-cryocooler technology, currently under development, will potentially be able to produce an extremely compact system for mobile terahertz imagers with video-rate speeds. FPAs with two or more pixels have a number of advantages over a single-pixel array. First, an object can be scanned faster by use of multiple pixels (image time is inversely proportional to the number of pixels in the array). Second, different pixels in the array can be operating at different frequencies simultaneously (by taking advantage of the high spectral resolution associated with heterodyne detectors). Third, signals with different polarizations can be detected simultaneously by use of different antenna structures for different pixels in the array. Fourth, correlation receivers employing two or more detectors on each pixel can improve sensitivity substantially. Fifth, taking advantage of the phase information to produce phase scans of the target can be implemented. In summary, this general architecture is well suited for construction of FPAs with a large number of pixels to produce terahertz imagers with superior sensitivities and speeds.

4. TERAHERTZ SPECTROSCOPY

Terahertz radiation can be used as a unique probe of complex gas molecules through its resonant interaction with their rotational energy transitions. We are developing terahertz spectrometers that can be utilized for non-destructive evaluation (NDE) of materials properties, scattering parameters, and noise of a wide range of systems. We are also developing the capability to perform spectroscopy on biological and chemical systems with unprecedented sensitivities and spectral resolutions. Terahertz spectroscopy of biological agents can play a major role in the study of the composition of biomaterials, changes of conformational states, molecular binding states, DNA hybridization, and the effect on cell processes, to name a few. Existing terahertz spectrometers lack the spectral resolution and sensitivity required to detect minute changes in the signal due to the processes listed above. Furthermore, spectroscopy of chemical agents can be used to characterize partially ionized plasmas in which gas molecules and molecular ions play a crucial role. Ion velocity and temperature measurements in hot plasmas have typically been performed with passive Doppler techniques in the visible or infrared optical range [9]. High-resolution Czerny-Turner optical spectrometers typically do not exceed $\lambda/\Delta\lambda \approx 10000$, leading to minimum velocity resolution of $c/10000 = 30$ km/s. The combination of the physical principles of optical Doppler spectroscopy with the extremely high frequency discrimination of terahertz heterodyne detection technology can potentially achieve high resolution velocity measurements (below meter per second) in industrial plasmas that have molecular resonances at these frequencies. The terahertz spectrum enables one to gain information about molecules that are central to applications involving plasma chemistry in a way that can not be achieved with optical and microwave diagnostics. Terahertz heterodyne HEB detection diagnostic technique, which takes advantage of high-resolution frequency discrimination, can potentially provide measurement data unavailable up to now.

Understanding the differences between heterodyne and direct detection as used in terahertz spectrometers (or terahertz imaging systems) is important. To promote understanding of the figures of merit of both detector technologies, a direct comparison is summarized in TABLE I. In general, in order to resolve magnitude and phase of a signal, a heterodyne detector should be chosen. A heterodyne detection system down-converts the signal into an intermediate frequency (IF) and requires a local oscillator source. For higher spectral resolution, heterodyne detector technology is preferable. The figure of merit for the sensitivity of direct detectors is the noise equivalent power (NEP), whereas noise temperature is used for heterodyne detectors. The distinction between *system* noise temperature and *receiver* noise temperature (for heterodyne detectors) is that the former includes the noise from the input source (ideally the vacuum fluctuations), whereas the latter includes the noise generated in the receiver only. Obviously, it is the system noise temperature that determines the sensitivity of a heterodyne detector system in a spectroscopic or imaging application. To compare the sensitivity of a heterodyne detector with that of a direct detector used in an active system (the target is illuminated), the noise temperature of the heterodyne detector has to be converted to noise equivalent power (see TABLE I). Detectors for passive systems are characterized by their noise equivalent difference in temperature (NE Δ T). TABLE I compares these figures of merit (NEP, NE Δ T) for existing detector technologies. In general, cooling a detector improves its sensitivity (i.e., lowers its intrinsic noise). We must also distinguish between “electrical” and “optical” NEP values. Electrical NEP values (NEP_e) are deduced from the current-voltage curve and the measured output noise, whereas optical NEP values are deduced from actual “optical” measurements on targets switched between known temperatures. To evaluate the system performance, the optical NEP (NEP_{opt}) should be used. The best performance reported for a direct detector at 4 K is for a thermally-isolated Nb thin bridge [10]. It was measured to yield $NEP_{opt}(\text{at } 1 \text{ s}) = 4 \cdot 10^{-13} \text{ W}/\sqrt{\text{Hz}}$ when the detector senses a very wide RF frequency range from 0.1 to 1.0 THz. For comparison, the NEP figure for a heterodyne HEB receiver with high spectral bandwidth (B) (10 kHz) (given in TABLE I, $2.8 \cdot 10^{-18} \text{ W}/\sqrt{\text{Hz}}$) is five orders of magnitude better than that of the best direct detector at 4 K for active systems. For passive

TABLE I
SUMMARY OF NOISE FIGURES OF MERIT

Heterodyne Detector	Direct Detector
<ul style="list-style-type: none"> ● <i>HEB (Hot Electron Bolometer) Mixer:</i> <i>DSB Noise temp. ~ 1000 K (at 4-6 K)</i> <i>Bandwidth 4 GHz</i> $\Delta T_{RMS} \geq 2T_{sys}/\sqrt{B\tau} = 100\text{mK}$ in 0.1 sec <i>and 32 mK in 1 s</i> ● <i>HEB (Hot Electron Bolometer) Mixer:</i> <i>DSB Noise temp. ~ 1000 K (at 4-6 K)</i> <i>Bandwidth 10 kHz</i> $\Delta T_{RMS} \geq 2T_{sys}/\sqrt{B\tau} = 20\text{ K}$ in 1 s ● <i>In terms of NEP:</i> $NEP_{HEB}(1\text{ s}) = k B \Delta T_{RMS}(4\text{GHz}) = 1.8 \cdot 10^{-15} \text{ W}/\sqrt{\text{Hz}}$ $NEP_{HEB}(1\text{ s}) = k B \Delta T_{RMS}(10\text{kHz}) = 2.8 \cdot 10^{-18} \text{ W}/\sqrt{\text{Hz}}$ $NE\Delta T_{HEB}(1\text{ s}) = \Delta T_{RMS} = 20\text{ K}$ $NE\Delta T_{HEB}(0.1\text{ s}) = \Delta T_{RMS} = 63\text{ K}$ 	<ul style="list-style-type: none"> ● <i>Nb direct detector:</i> <i>Frequency about 100 GHz:</i> <i>Active system (IMPATT at 1 W peak)</i> $NEP_{Nb}(1\text{ s}) = 5 \cdot 10^{-11} \text{ W}/\sqrt{\text{Hz}}$ at room temp. $Improved\ NEP_{Nb}(1\text{ s}) = 5 \cdot 10^{-12} \text{ W}/\sqrt{\text{Hz}}$ at room temp. <i>Frequency about 100-1000 GHz:</i> $NEP_{Nb}(1\text{ s}) = 4 \cdot 10^{-13} \text{ W}/\sqrt{\text{Hz}}$ (at 4 K) [10] $NE\Delta T_{Nb} = NEP_{Nb}/(k B)$ in 1 s integration time $NE\Delta T_{Nb}(1\text{ s}) = 32\text{ mK}$ <i>Assume spectral bandwidth of 10 kHz:</i> <i>For $NEP_{Nb} = 4 \cdot 10^{-13} \text{ W}/\sqrt{\text{Hz}}$, $NE\Delta T_{Nb}(1\text{ s}) = 2.9 \cdot 10^5\text{ K}$</i> $NE\Delta T_{Nb}(0.1\text{ s}) = 9.2 \cdot 10^6\text{ K}$

systems, we should instead compare the NE Δ T of an HEB with the above Nb direct detector. To perform passive spectroscopy with high spectral resolution, a drastic narrowing of the bandwidth is required and will lead to extremely low sensitivity (NE Δ T of thousands of kelvins). Such a wide frequency range would not be useful in a passive terahertz imaging system requiring high spatial resolution, because the beamwidth, sensed by the optics, would vary by a factor of ten over the frequency range (determined by the aperture size in wavelengths). Furthermore, direct detectors, with the sensitivity of those in [10], have not been demonstrated at frequencies higher than 1 THz, whereas HEB detectors can be used over the entire terahertz range with similar performance. One clear advantage of the direct detectors is the lack of LO source requirement. Nevertheless, the demonstrated performance of heterodyne detectors, in the terahertz spectrum, makes them superior for both active and passive spectroscopic and imaging applications requiring high sensitivities and high spectral and spatial resolutions.

REFERENCES

1. E. Gerecht, et al., "NbN Hot Electron Bolometric Mixers, a New Technology for Low-Noise THz Receivers," IEEE Trans. Microw. Theory Tech., vol. 47, no. 12, pp. 2519–2527, Dec. 1999.
2. D. F. Filipovic, S. S. Gearhart, and G. M. Rebeiz, "Double-Slot Antenna on Extended Hemispherical and Elliptical Silicon Dielectric Lenses," IEEE Trans. Microw. Theory Tech., vol. 41, no. 10, pp. 1738–1749, Oct. 1993.
3. E. Gerecht, D. Gu, X. Zhao, J. Nicholson, F. Rodriguez- Morales, and S. Yngvesson, "Development of NbN Terahertz HEB Mixers Coupled Through Slot Ring Antennas", 15th Intern. Symp. Space THz Technol., Northampton, MA, April 27-29, 2004.

4. R. Köhler, A. Tredicucci, F. Beltram, H. E. Beer, E. H. Linfield, A. G. Davies, D. A. Ritchie, R. C. Iotti, and F. Rossi, "Terahertz semiconductor-heterostructure laser," *Nature*, vol. 417, no. 6885, pp. 156-159, May 2002.
5. Virginia Diodes, Inc, <http://www.virginiadiodes.com/multipliers.htm>
6. F. Rodriguez-Morales, S. Yngvesson, R. Zannoni, E. Gerecht, D. Gu, N. Wadefalk, and J. Nicholson, "Development of Integrated HEB/MMIC Receivers for Near-Range Terahertz Imaging," *IEEE Trans. Microw. Theory Tech.* vol. 54, no. 6, Jun. 2006.
7. J. Randa, E. Gerecht, D. Gu, and R. Billinger, "Precision Measurement Method for Cryogenic Amplifier Noise Temperatures Below 5 K," *IEEE Trans. Microw. Theory Tech.*, vol. 54, no. 3, pp. 1180-1189, Mar. 2006.
8. D. Gu, E. Gerecht, F. Rodriguez-Morales, and S. Yngvesson, "Two-Dimensional Terahertz Imaging System Using Hot Electron Bolometer Technology", 17th Intern. Symp. Space THz Technol., Paris, France, April 10-12, 2006.
9. T. Munsat et al., "Microwave imaging reflectometer for TEXTOR", *Rev. Sci. Instrum.* 74, 1426-1432, 2003.
10. A. Luukanen, et al., "An Ultra-Low Noise Superconducting Antenna-Coupled Microbolometer With a Room-Temperature Read-Out," *IEEE Microw. Wireless Compon. Lett.*, Vol 16, No. 8, August 2006.